Chemical Science

ROYAL SOCIETY OF CHEMISTRY

EDGE ARTICLE

View Article Online
View Journal | View Issue

Cite this: *Chem. Sci.*, 2020, **11**, 11214

All publication charges for this article have been paid for by the Royal Society of Chemistry

Received 9th August 2020
Accepted 16th September 2020

DOI: 10.1039/d0sc04385k

rsc.li/chemical-science

Revitalizing silver nanocrystals as a redox catalyst by modifying their surface with an isocyanide-based compound†

Shi Shi,[a] Yadong Zhang,[b] Jaewan Ahn[a] and Dong Qin *[a]

Silver is an excellent catalyst for oxidation reactions such as ethylene epoxidation, but it shows limited activity toward reduction reactions. Here we report a strategy to revitalize Ag nanocrystals as a redox catalyst for the production of an aromatic azo compound by modifying their surface with an isocyanide-based compound. We also leverage *in situ* fingerprint spectroscopy to acquire molecular insights into the reaction mechanism by probing the vibrational modes of all chemical species at the catalytic surface with surface-enhanced Raman spectroscopy. We establish that binding of isocyanide to Ag nanocrystals makes it possible for Ag to extract the oxygen atoms from the nitro-groups of nitroaromatics and then use these atoms to oxidize isocyanide to isocyanate. Concurrently, the coupling between two adjacent deoxygenated nitroaromatic molecules leads to the formation of an aromatic azo compound.

Introduction

Silver nanocrystals have found widespread use as a catalyst for ethylene epoxidation, one of the key processes to produce ethylene oxide for the synthesis of ethylene glycol, detergents, and many other chemicals.[1–4] Nevertheless, Ag shows limited catalytic activity toward reduction reactions when compared to platinum-group metals (PGMs) such as Pt, Pd, Rh, and Ir.[5–9] One approach to overcome this limitation is to decorate the surface of Ag nanocrystals with a PGM for the fabrication of Ag-based bimetallic nanocrystals. To this end, we and other groups have demonstrated the synthesis of Ag@M (M = Pt, Pd, Au, and Rh) nanocrystals with a core-frame, core–shell, or core-satellite structure.[10–16] The successful development of such bimetallic nanocrystals also offers a probe with integrated plasmonic and catalytic activities for catalyzing a chemical reaction while reporting on the chemical species involved through *in situ* surface-enhanced Raman spectroscopy (SERS).[17–19] For example, we demonstrated that Ag–Pd core-frame nanocubes could serve as a dual-catalytic system, with the Pd and Ag components catalyzing step-wise, sequential reduction and oxidation reactions, respectively.[11,20] Significantly, we could monitor and analyze the Pd-catalyzed reduction of 4-nitrothiophenol (4-NTP) to 4-aminothiophenol (4-ATP) by $NaBH_4$ and the subsequent Ag-catalyzed oxidation of 4-ATP to *trans*-4,4′-dimercaptoazobenzene (*trans*-DMAB) by O_2 from air by fingerprinting the vibrational modes of these species *in situ* using SERS.

Another avenue to expand the catalytic capacity of Ag nanocrystals is to modify their surface by introducing an organic ligand. Although organic ligands are often used to stabilize the particles during their colloidal synthesis, it has long been recognized that the organic ligands remaining on the surface could relentlessly "poison" catalytic particles by simply blocking the active sites.[21–25] Here we demonstrate that organic ligands can have a positive impact on the properties of catalytic particles. Specifically, we discover that an isocyanide compound can adsorb on the surface of Ag nanocubes to enable the Ag-catalyzed redox reaction between isocyanide and nitroaromatic molecules toward the production of an aromatic azo compound under ambient conditions. Because the binding of the isocyanide group (–NC) to Ag is similar to that of carbon monoxide (CO),[26] we argue that isocyanide can adsorb onto Ag through σ donation.[27,28] When 4-NTP molecules are introduced onto the isocyanide-modified surface through Ag-thiolate linkage, a redox couple will be formed on the surface of Ag nanocubes. We hypothesize that the nitro group of the adsorbed 4-NTP can react with the modified Ag surface for the creation of atomic oxygen, followed by the oxidation of isocyanide to isocyanate.[29] Simultaneously, the coupling between two adjacent deoxygenated nitroaromatic molecules leads to the

[a]*School of Materials Science and Engineering, Georgia Institute of Technology, Atlanta, Georgia 30332, USA. E-mail: dong.qin@mse.gatech.edu*

[b]*School of Chemistry and Biochemistry, Georgia Institute of Technology, Atlanta, Georgia 30332, USA*

† Electronic supplementary information (ESI) available: Experimental details, a TEM image of Ag nanocubes, the particle size distribution histogram of the Ag nanocubes, a SERS spectrum in the range from 500 to 3500 cm^{-1} collected from an ethanolic suspension of Ag nanocubes and 1,4-PDI, a SERS spectrum in the range from 1663.74 to 2679.38 cm^{-1} collected from a suspension of Ag nanocubes in 1,4-PDI, followed by the addition of a 4-NTP solution in ethanol, a Raman spectrum recorded from the 4-NTP solution in ethanol and time-elapsed SERS spectra collected from an ethanolic suspension of Ag nanocubes and 4-NTP before and after the addition of aqueous $NaBH_4$, and a table of the SERS and ordinary Raman shifts of 1,4-PDI and their assignments. See DOI: 10.1039/d0sc04385k

formation of an aromatic azo compound.[30,31] To gain molecular insights into the catalytic process, we leverage *in situ* SERS to track the chemical species involved in this redox reaction by following the stretching frequency of the –NC band on Ag ($\nu_{NC(Ag)}$), the –NCO stretching band (ν_{NCO}) of isocyanate, as well as other characteristic bands associated with 4-NTP and *trans*-DMAB.

Results and discussion

In this study, we used Ag nanocubes with an average edge length of 37.7 ± 2.6 nm (Fig. S1†). Fig. 1 illustrates how spectroscopy fingerprinting can be used to decipher the Ag-catalyzed redox reaction of 4-NTP on the Ag nanocubes modified by 1,4-phenylene diisocyanide (1,4-PDI). In the first step, when 1,4-PDI molecules bind to a Ag surface through both of their –NC groups in the lay-flat configuration, with the long molecular axis parallel to the surface, we will detect the Ag-bound N–C stretching band ($\nu_{NC(Ag)}$) at 2180 cm^{-1} and the C–H out-of-plane bending band ($\delta_{CH,out\text{-}of\text{-}plane}$) at 830 cm^{-1}.[26,32] Alternatively, when the binding only involves one of their –NC groups, with the long molecular axis parallel to the surface normal in an upright configuration, we will observe the $\nu_{NC(Ag)}$ at 2180 cm^{-1}, in addition to the free N–C stretching band ($\nu_{NC(free)}$) and C–H stretching band (ν_{CH}) at 2127 and 3074 cm^{-1}, respectively. In both cases, the –NC group binds to Ag through σ donation.

In the second step, we investigate the redox reaction between 1,4-PDI and 4-NTP co-adsorbed on the Ag surface. We argue that the 4-NTP molecules can adsorb onto the surface by occupying the vacant sites through the formation of Ag–thiolate linkage.[33] It is also possible that 4-NTP molecules could replace some of the pre-adsorbed 1,4-PDI due to stronger bonding when the concentration of 4-NTP is comparable to or higher than that of 1,4-PDI in the reaction solution.[34] In particular, when the 4-NTP

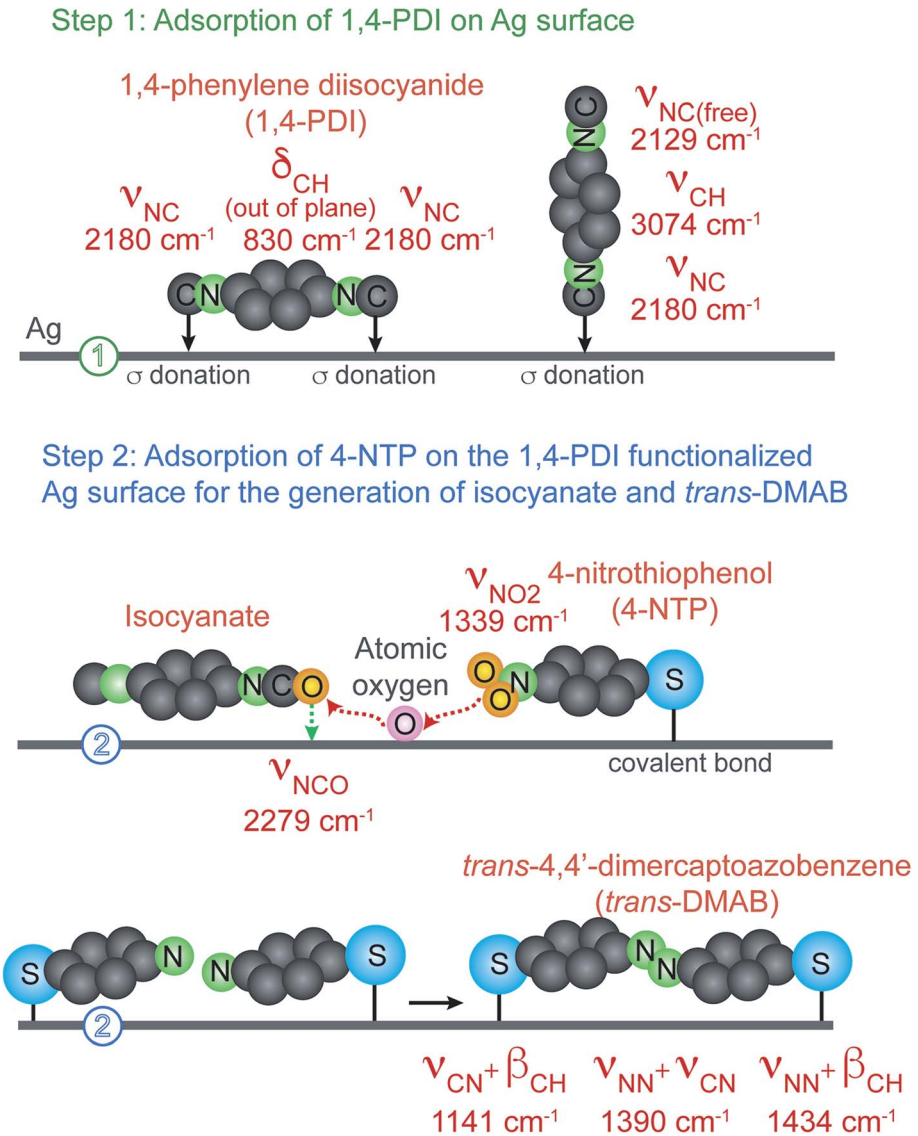

Fig. 1 Schematic illustration of the proposed Ag-catalyzed oxidation of isocyanide to isocyanate for the reduction of 4-NTP to *trans*-DMAB on the Ag surface.

molecules are oriented with their long molecular axis parallel to the surface, they can be reduced because the oxygen atoms of nitro-groups can be extracted by the modified Ag surface and subsequently used to oxidize isocyanide to isocyanate. The decrease of the $\nu_{NC(Ag)}$ band of 1,4-PDI at 2180 cm^{-1} and the appearance of the –NCO stretching band (ν_{NCO}) of the isocyanate species at 2280 cm^{-1} would offer direct evidence to support the occurrence of this oxidation reaction. Concurrently, the coupling between two adjacent deoxygenated 4-NTP molecules will lead to the formation of *trans*-DMAB, which can be detected using the $\nu_{CN} + \beta_{CH}$, $\nu_{NN} + \nu_{CN}$, and $\nu_{NN} + \beta_{CH}$ bands located at 1141, 1390, and 1434 cm^{-1}, respectively.[35] The appearance of vibrational peaks indexed to *trans*- rather than *cis*-DMAB will further support our argument about a lay-flat instead of an upright configuration for the 4-NTP molecules adsorbed on the Ag surface.[36]

In a standard protocol, we dispersed Ag nanocubes in a 1,4-PDI solution (10^{-4} M) in ethanol, followed by the addition of a 4-NTP solution (10^{-5} M) in ethanol at a molar ratio of 10 : 1 between 1,4-PDI and 4-NTP. Aliquots were sampled from the reaction mixture at different time points for Raman analysis. We assume that the SERS signals mostly originated from the molecules in proximity to the hot spots that were located at the edges of individual Ag nanocubes.[37] Fig. 2 shows a series of Raman/SERS spectra collected by withdrawing samples from the mixture at different time points. At the starting point, we collected a Raman spectrum from the 1,4-PDI/ethanol solution, from which we only identified the Raman peaks associated with ethanol (marked by open stars).[38] In fact, we could use the ethanol peak at 883 cm^{-1} (ν_{CC}) as a reference to monitor the change in peak intensity for Raman bands in the time-lapsed SERS spectra because the position and peak intensity of this band remained essentially the same in the entire course of a SERS experiment. At $t = 5$ min post the addition of Ag nanocubes, we resolved the SERS peaks of 1,4-PDI (marked by green dots) at 1164, 1203, 1596, and 2180 cm^{-1}, with their assignments to C–H in-plane bending ($\delta_{CH,in\text{-}plane}$), C–NC stretching ($\nu_{C\text{–}NC}$), C–C stretching ($\nu_{CC}$), and N–C stretching ($\nu_{NC(Ag)}$) bands, respectively (see Table S1†). The weak peak at 2129 cm^{-1} was assigned to the unbonded N–C stretching peak ($\nu_{NC(free)}$). At $t =$ 60 min, the SERS peaks of 1,4-PDI remained largely the same in terms of position. We noticed that the intensity ratio between the 1,4-PDI $\nu_{NC(Ag)}$ peak at 2180 cm^{-1} and the ethanol ν_{CC} band at 883 cm^{-1} was slightly increased from 3.50 to 4.24, suggesting the adsorption of more 1,4-PDI molecules onto the surface of Ag nanocubes. It is also possible that a stronger interaction between 1,4-PDI and the Ag surface could enhance the SERS signal through chemical enhancement.[39]

To investigate the orientation of the adsorbed 1,4-PDI relative to the Ag surface, we collected another SERS spectrum in

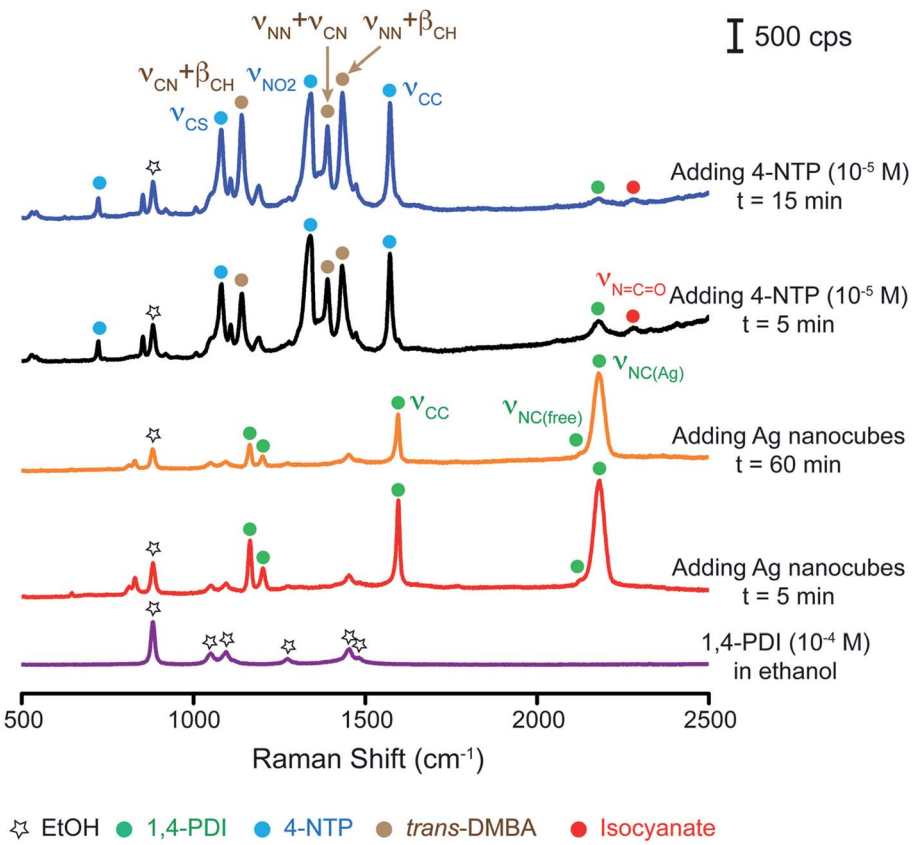

Fig. 2 Raman spectrum recorded from a 1,4-PDI solution (10^{-4} M) in ethanol and time-elapsed SERS spectra collected at different time points from an ethanolic suspension of Ag nanocubes and 1,4-PDI before and after the addition of 4-NTP solution in ethanol (10^{-5} M).

the range of 500–3500 cm^{-1}. As shown in Fig. S2,† we resolved peaks appearing at 830 and 3074 cm^{-1}, with their assignments to the $\delta_{CH,out\text{-}of\text{-}plane}$ and ν_{CH} bands of 1,4-PDI, respectively. Taken together, the SERS data suggested that the adsorbed 1,4-PDI took both the lay-flat and upright configurations (Fig. 1, step 1). Similar to what was demonstrated by Whitesides and coworkers in previous studies for the adsorption of alkanethiolates on a Au or Ag thin film,[33] we argue that adsorbed 1,4-PDI would prefer to lie flat on the surface in the early stage of adsorption, followed by transition into the upright configuration to maximize the coverage density of the adsorbed molecules at a typical time scale of about 60 min.

After the introduction of 4-NTP for 5 min, the SERS spectrum shows the appearance of peaks at 1080, 1339, and 1572 cm^{-1} for the ν_{CS}, ν_{NO_2}, and ν_{CC} bands of 4-NTP, respectively, confirming the attachment of 4-NTP to the surface of the Ag nanocubes. We also observed the characteristic peaks of *trans*-DMAB at 1141, 1390, and 1434 cm^{-1} for the $\nu_{CN} + \beta_{CH}$, $\nu_{NN} + \nu_{CN}$, and $\nu_{NN} + \beta_{CH}$ bands, respectively, indicating the reduction of 4-NTP to *trans*-DMAB. Because we did not observe the signature bands of *cis*-DMAB located at 621 cm^{-1} and 778 cm^{-1},[36] we believe that that it was not a predominant product. In comparison, all the bands associated with 1,4-PDI showed a significant drop in intensity. Interestingly, a weak peak appeared at ~2280 cm^{-1} (marked by a red dot), with its possible assignment to the ν_{NCO} band of the isocyanate group.[29] To further verify the presence of the ν_{NCO} band, we recorded anther SERS spectrum using the *static* mode (see details in the Experimental section). As shown in Fig. S3,† we clearly resolved both the $\nu_{NC(Ag)}$ band of 1,4-PDI at 2178 cm^{-1} and the ν_{NCO} band of the isocyanate group at 2279 cm^{-1}, confirming the conversion of isocyanide to isocyanate. It is worth mentioning that the weak ν_{NCO} band of isocyanate may suggest the weak binding of this molecule to Ag. As such, we argue that isocyanate molecules could readily leave the Ag surface, making it possible for the remaining isocyanide molecules in the solution to continuously adsorb onto the Ag surface. In a sense, it is feasible to sustain the catalytic activity of the isocyanide-modified Ag nanocubes until 1,4-PDI is completely consumed in the reaction solution. Additionally, we believe that the peak located at 2576 cm^{-1} could be assigned to the S–H stretching band of free 4-NTP.[40] Likely, some of the 4-NTP molecules could be situated in proximity to the SERS hot spots without forming the Ag–thiolate bond. As the reaction progressed to $t = 15$ min, the spectrum remained essentially the same except for a slight increase in intensity for the peaks of *trans*-DMAB. We noticed that the intensity ratio between the peak of *trans*-DMAB $\nu_{NN} + \beta_{CH}$ at 1434 cm^{-1} and the peak of ethanol ν_{CC} at 883 cm^{-1} was increased from 2.61 to 3.59, indicating more production of *trans*-DMAB. Similar to the case of 1,4-PDI, the stronger interaction between *trans*-DMAB molecules and Ag could also contribute to an increase in SERS signal due to chemical enhancement.[39] Altogether, these results support our hypothesis that 4-NTP can be reduced by 1,4-PDI on a Ag surface for the generation of *trans*-DMAB and isocyanate species (Fig. 1, step 2).

We performed two sets of control experiments to understand the essential role played by 1,4-PDI modified Ag nanocubes in support of the Ag-catalyzed redox reaction. In the first set, we excluded the participation of 1,4-PDI by directly dispersing the Ag nanocubes in the 4-NTP/ethanol solution (10^{-5} M) while keeping all other experimental parameters the same as the standard protocol. Fig. S4† shows a series of Raman/SERS spectra collected by withdrawing samples from the ethanol mixture at different time points. Initially, the Raman spectrum of the 4-NTP solution showed the peaks of ethanol only. At $t =$ 15 min post the addition of Ag nanocubes, we identified the ν_{CS}, ν_{NO_2}, and ν_{CC} bands of 4-NTP at 1082, 1343, and 1572 cm^{-1}, respectively, confirming the adsorption of 4-NTP onto the Ag surface. By $t = 30$ min, the three characteristic peaks of 4-NTP remained at the same positions and no new peaks appeared in the SERS spectrum. We then introduced aqueous $NaBH_4$ (0.1 mg mL^{-1}) into the reaction mixture. At $t = 5$ min after the introduction of $NaBH_4$, the SERS spectrum showed no emerging three characteristic peaks of *trans*-DMAB and we only resolved the two major peaks of 4-NTP due to the significant decrease in SERS signal. The SERS spectrum remained essentially the same, except for a continuous decrease in peak intensity up to $t =$ 30 min. We argue that such a drop in SERS signal can be attributed to the dilution factor (see the Experimental section for details), as well as the desorption of some 4-NTP due to a stronger binding of BH_4^- to the Ag surface.[41,42] Taken together, these results confirmed that Ag nanocubes are not a good catalyst for the reduction of 4-NTP, consistent with our previous findings.[11]

In the second set of experiments, we reversed the order of introducing 1,4-PDI and 4-NTP into the suspension of Ag nanocubes. Fig. 3A shows a series of Raman/SERS spectra recorded at different time points. At the beginning, we collected a Raman spectrum from the 4-NTP solution (10^{-5} M) and only observed the peaks of ethanol. At $t = 5$ min after the addition of Ag nanocubes, we observed the three signature peaks of 4-NTP and these peaks remained essentially the same up to $t = 60$ min. Upon introducing the 1,4-PDI solution in ethanol (10^{-4} M) and waiting for 5 min, we only resolved the small ν_{CC} band of 1,4-PDI while other bands remained invisible, suggesting the limited number of 1,4-PDI molecules adsorbed onto the Ag surface. Although the characteristic bands of 4-NTP remained at the same positions, their intensities dropped. For example, we noticed that the intensity of the ν_{CC} band of 4-NTP decreased by almost 6 fold. There are two possible reasons for such a decrease in the SERS signal of 4-NTP. Firstly, we reduced the number of nanoparticles for SERS measurements due to a dilution factor of two (see the Experimental section for details). Secondly, we argue that 1,4-PDI molecules could replace some of the 4-NTP adsorbed on the surface of Ag nanocubes when the concentration of 1,4-PDI (10^{-4} M) is 10-fold as high as that of 4-NTP in the reaction solution (10^{-5} M).[34] At $t = 15$ min, we resolved both ν_{CC} and $\nu_{NC(Ag)}$ bands of 1,4-PDI in the SERS spectrum, with an intensity ratio of 0.08 between the 1,4-PDI $\nu_{NC(Ag)}$ peak and the ethanol ν_{CC} band. This result suggests that some 1,4-PDI molecules could indeed be adsorbed onto the Ag surface pre-covered with 4-NTP. Interestingly, the ν_{CC} band of 4-NTP showed almost a 3-fold increase in peak intensity. As more 1,4-PDI molecules occupied the surface, we suspect that the SERS signal could be enhanced due to an

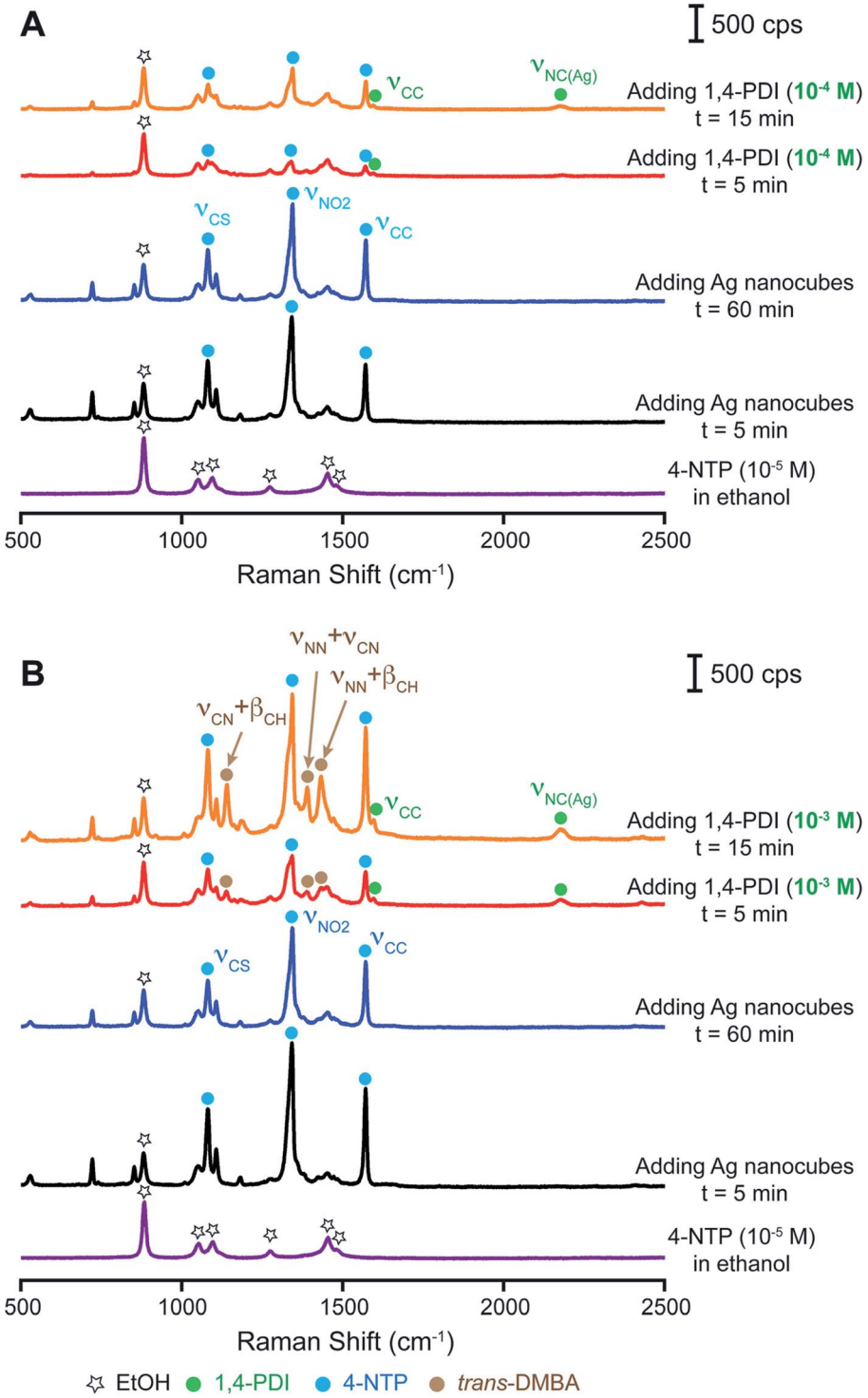

Fig. 3 Raman spectrum recorded from a 4-NTP solution (10^{-5} M) in ethanol and time-elapsed SERS spectra collected from an ethanolic suspension of Ag nanocubes and 4-NTP before and after the addition of 1,4-PDI solution in ethanol at (A) 10^{-4} M and (B) 10^{-3} M.

increased interaction between 1,4-PDI and the Ag surface by chemical enhancement.[39] However, we could not detect any vibrational bands associated with *trans*-DMAB, indicating no chemical reduction for 4-NTP. In this case, we hypothesize that the initial adsorption of 4-NTP on the Ag nanocubes could greatly limit the number of 1,4-PDI molecules adsorbed onto the surface,[34] making it difficult to initiate the Ag-catalyzed redox reaction. Our results also suggest that the free 1,4-PDI molecules in the reaction mixture were unable to contribute to the reduction of 4-NTP on the Ag surface.

To further validate our hypothesis, we performed another set of measurements by increasing the concentration of 1,4-PDI

from 10^{-4} M to 10^{-3} M while keeping all other parameters constant. As shown in Fig. 3B, the time-elapsed SERS spectra were essentially the same as those shown in Fig. 3A upon the introduction of Ag nanocubes into the 4-NTP/ethanol solution (10^{-5} M). However, 5 min post the introduction of 10^{-3} M 1,4-PDI/ethanol solution, both the ν_{CC} and $\nu_{NC(Ag)}$ bands of 1,4-PDI appeared in the SERS spectrum, with the intensity ratio between the 1,4-PDI $\nu_{NC(Ag)}$ peak and the ethanol ν_{CC} band increasing to 0.14. Obviously, more 1,4-PDI molecules were adsorbed on the surface of Ag nanocubes as the concentration of 1,4-PDI was increased from 10^{-4} to 10^{-3} M. Additionally, the spectrum shows the characteristic bands of 4-NTP and *trans*-DMAB, suggesting the reduction of 4-NTP by isocyanide. It was also found that the intensity of the ν_{CC} band of 4-NTP was reduced by 2 times, not as significant as the case shown in Fig. 3A. We argue that the presence of *trans*-DMAB could increase the SERS signal through chemical enhancement owing to the favorable interaction between *trans*-DMAB and the Ag surface.[39,43] At $t = 30$ min, the SERS spectrum remained essentially the same while the SERS signal became stronger, likely due to the production of more *trans*-DMAB on the surface. In this case, the intensity ratio between the 1,4-PDI $\nu_{NC(Ag)}$ peak and the ethanol ν_{CC} band further increased to 0.24. It is worth mentioning that the ν_{NCO} band of the isocyanate group was too

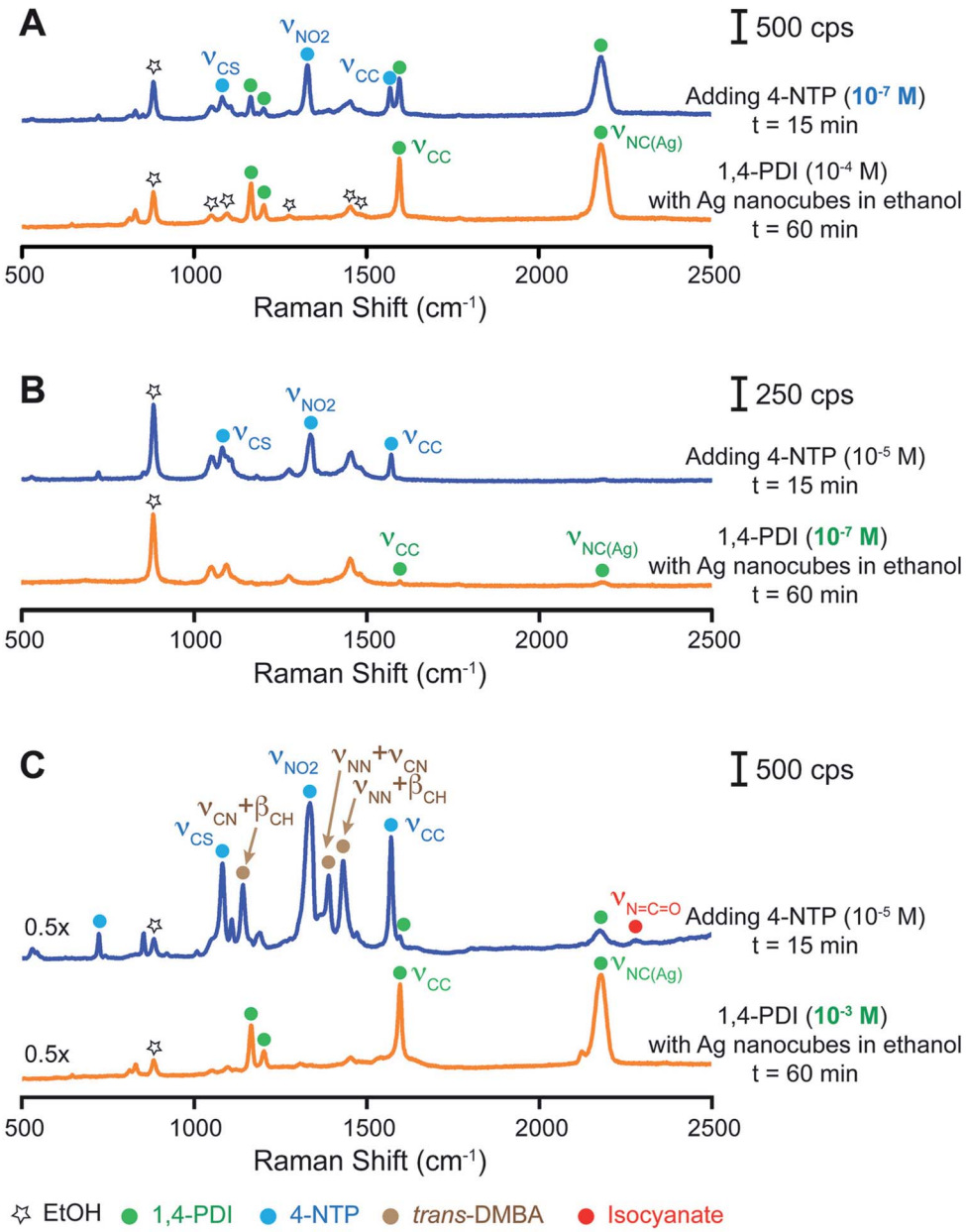

Fig. 4 SERS spectrum collected from the ethanolic suspension of Ag nanocubes and 1,4-PDI at $t = 60$ min and another spectrum recorded at $t =$ 15 min after the addition of 4-NTP solution in ethanol. The concentrations of 1,4-PDI and 4-NTP in ethanol were (A) 10^{-4} M and 10^{-7} M, (B) 10^{-7} M and 10^{-5} M, and (C) 10^{-3} M and 10^{-5} M, respectively.

weak to be resolved in the SERS spectrum. Taken together, we argue that it is essential to co-adsorb an adequate number of 1,4-PDI molecules on the Ag surface in order to trigger the reduction of 4-NTP to *trans*-DMAB.

Based on the above results, we argue that the co-adsorbed 1,4-PDI and 4-NTP would create a redox couple on the Ag surface, making Ag a redox catalyst for the oxidation of isocyanide to isocyanate and reduction of 4-NTP to *trans*-DMAB. Under this assumption, we speculate that the coverage densities of both 1,4-PDI and 4-NTP on the Ag surface would play a vital role in enabling this redox reaction. Although it is still impossible to quantify the numbers of 1,4-PDI and 4-NTP molecules adsorbed on the surface of Ag nanocubes, we made an attempt to maneuver the coverage densities of these two adsorbates by varying their concentrations in the solutions while fixing the number of Ag nanocubes in the ethanol suspension. Specifically, we collected a SERS spectrum at $t = 60$ min after the introduction of Ag nanocubes into the 1,4-PDI/ethanol solution and another spectrum at $t = 15$ min after the addition of 4-NTP/ethanol solution. Fig. 4 shows three sets of SERS data. In the first scenario, we kept the concentration of 1,4-PDI at 10^{-4} M while decreasing the concentration of 4-NTP from 10^{-5} M to 10^{-7} M to obtain a molar ratio of 1,4-PDI to 4-NTP at 1000 : 1. Fig. 4A gives the SERS spectrum of Ag nanocubes dispersed in 10^{-4} M 1,4-PDI/ethanol solution, which is similar to the observation in Fig. 2 at the time point of 60 min. The intensity ratio between the 1,4-PDI $\nu_{NC(Ag)}$ peak and the ethanol ν_{CC} band was at 2.3. After adding the 10^{-7} M 4-NTP/ethanol solution and waiting for 15 min, the three characteristic peaks of 4-NTP emerged while the bands of 1,4-PDI remained in the SERS spectrum. The intensity ratio between the 1,4-PDI $\nu_{NC(Ag)}$ peak and the ethanol ν_{CC} band dropped to 1.6. Such a decrease in peak intensity could result from the interplay between the dilution effect for the decrease in SERS (see the Experimental section for details) and the chemical enhancement effect of the 4-NTP adsorbed on Ag for the increase in SERS.[39,44] We did not find any vibrational bands associated with *trans*-DMAB in the spectrum. This result suggests that there was no reduction of 4-NTP to *trans*-DMAB when the Ag surface was predominantly covered with 1,4-PDI molecules, with a limited number of 4-NTP molecules.

In the second scenario, we decreased the concentration of 1,4-PDI from 10^{-4} to 10^{-7} M while keeping the concentration of 4-NTP at 10^{-5} M to attain a molar ratio of 1,4-PDI to 4-NTP at 1 : 100. Fig. 4B shows the SERS spectrum of Ag nanocubes suspended in 10^{-7} M 1,4-PDI solution in ethanol at the time point of 60 min, from which we identified both the ν_{CC} and $\nu_{NC(Ag)}$ bands of 1,4-PDI. In comparison with those shown in Fig. 4A, these two bands exhibited a much weaker intensity owing to the limited number of 1,4-PDI molecules adsorbed on the Ag surface. The intensity ratio between the 1,4-PDI $\nu_{NC(Ag)}$ peak and the ethanol ν_{CC} band was only 0.05. It is worth noting that the overall SERS signal became weaker when a limited number of 1,4-PDI molecules adsorbed on the surface, consistent with our prior argument on the role of interaction between 1,4-PDI and Ag in contributing to the chemical enhancement of SERS. After the introduction of 10^{-5} M 4-NTP solution in ethanol, the SERS spectrum only showed the characteristic bands of 4-NTP, and no bands associated with either 1,4-PDI or *trans*-DMAB were observed. Because 4-NTP would certainly replace 1,4-PDI on Ag due to stronger bonding when the concentration of 4-NTP (10^{-5} M) was 100-fold larger than that of 1,4-PDI in the reaction solution (10^{-7} M),[34] we argue that the Ag surface would be mostly covered by 4-NTP, with a very limited number of 1,4-PDI molecules. As a result, there is no reduction of 4-NTP to *trans*-DMAB, consistent with our prior result presented in Fig. 3A.

In the third scenario, we increased the concentration of 1,4-PDI from 10^{-4} to 10^{-3} M while maintaining the concentration of 4-NTP at 10^{-5} M to achieve a molar ratio of 1,4-PDI to 4-NTP at 100 : 1. As shown in Fig. 4C, the SERS signal of 1,4-PDI became stronger than those shown in Fig. 4A and B. The intensity ratio between the 1,4-PDI $\nu_{NC(Ag)}$ peak and the ethanol ν_{CC} band was as high as 5.8. Again, we argue that such an increase in SERS signal could be attributed to the chemical enhancement arising from the increased number of 1,4-PDI molecules adsorbed on the Ag surface.[39] After the addition of 4-NTP, we noticed that the intensity ratio between the 1,4-PDI $\nu_{NC(Ag)}$ peak and the ethanol ν_{CC} band was significantly reduced to 0.84 while we resolved the ν_{NCO} band of the isocyanate group. Additionally, the characteristic bands of 4-NTP and *trans*-DMAB appeared in the SERS spectrum. In fact, this set of data is consistent with those shown in Fig. 2. Collectively, these three sets of studies strongly support our proposed mechanism in which the numbers of both 1,4-PDI and 4-NTP absorbates on the Ag surface play a vital role in creating a redox couple on Ag nanocubes for enabling the oxidation of isocyanide toward isocyanate and the reduction of 4-NTP to *trans*-DMAB.

To further validate our proposed mechanism, we replaced 1,4-PDI with 4,4′-biphenyl diisocyanide (BPDI) while keeping all other experimental parameters the same. BPDI has a linear conformation similar to that of 1,4-PDI with the two benzene planes.[45,46] Fig. 5 shows a series of Raman/SERS spectra collected at different time points. At $t = 5$ min post the introduction of Ag nanocubes into a BPDI solution (10^{-4} M) in ethanol, we identified the emergence of peaks at 1171, 1283, 1601, and 2182 cm^{-1}, which can be assigned to the δ_{CH}, ν_{C-NC}, ν_{CC}, and $\nu_{NC(Ag)}$ bands of BPDI, respectively.[28,47,48] By comparing the $\nu_{NC(Ag)}$ peak intensity of BPDI with that of 1,4-PDI shown in Fig. 2 at the same concentration of 10^{-4} M, we noticed that the SERS signal of BPDI was much stronger. Likely, such an enhancement in Raman signal can be attributed to the larger π-conjugation system of BPDI for promoting a stronger interaction between the molecules and the Ag surface, consistent with our argument in the context of chemical enhancement. The SERS spectrum remained essentially the same over a period of at least 60 min. Upon the addition of a 4-NTP/ethanol solution (10^{-5} M) and waiting for 5 min, we observed a significant decrease in intensity for those bands associated with BPDI. However, we still detected the ν_{CC} and $\nu_{NC(Ag)}$ bands of BPDI, as well as a weak peak at 2281 cm^{-1} that corresponds to the ν_{NCO} band of isocyanate due to the excellent SERS signal. On the other hand, we observed the predominance of the SERS peaks of *trans*-DMAB, together with the peaks associated with 4-NTP.

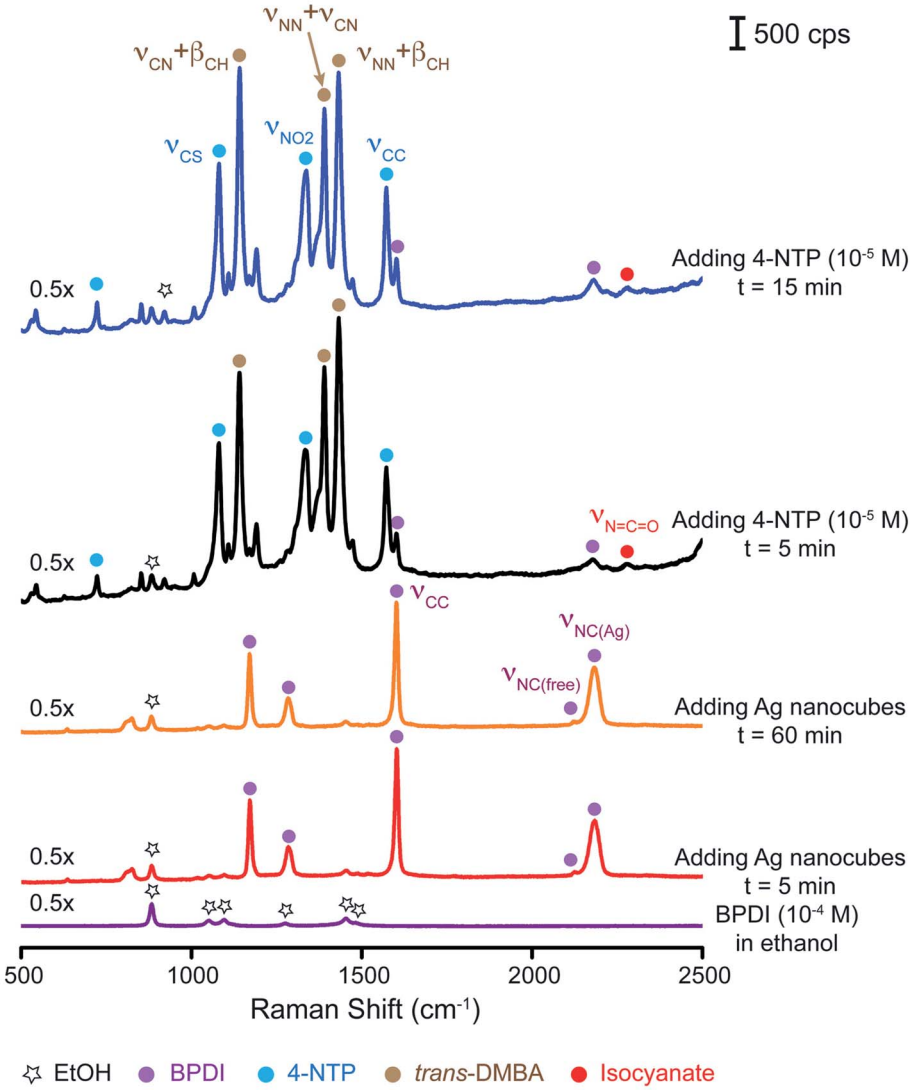

Fig. 5 Raman spectrum recorded from a BPDI solution (10^{-4} M) in ethanol and time-elapsed SERS spectra collected at different time points from an ethanolic suspension of Ag nanocubes and BPDI before and after the addition of 4-NTP solution in ethanol (10^{-5} M).

The SERS spectrum showed very little change in the next 10 min, only displaying a slight increase in the SERS signal. We noticed that the intensity ratio between the *trans*-DMAB ν_{NN}+-β_{CH} peak and the ethanol ν_{CC} band was increased to 14.5, almost 4 times as high as that shown in Fig. 2. This result suggests that BPDI with a larger π-conjugation system would become a better candidate to support the reduction of 4-NTP to *trans*-DMAB at the expense of isocyanide to isocyanate.

Conclusion

In summary, we have demonstrated the use of an isocyanide-based compound to modify the surface of Ag nanocubes for revitalizing Ag as a redox catalyst toward the production of an aromatic azo compound under ambient conditions. In a typical process, we dispersed Ag nanocubes in an ethanol solution containing 1,4-PDI, followed by the addition of 4-NTP solution in ethanol. We collected aliquots from the reaction solution at different reaction time points for analysis by Raman spectroscopy. Our SERS results confirmed that 1,4-PDI molecules can adsorb on Ag in both the lay-flat and upright configurations, with two –NC groups and a single –NC group binding to Ag, respectively. After the co-adsorption of 4-NTP molecules, we observed the decrease of the $\nu_{NC(Ag)}$ band of 1,4-PDI and the appearance of the ν_{NCO} band of isocyanate, demonstrating the oxidation of isocyanide to isocyanate. Concomitantly, we observed the vibrational bands associated with *trans*-DMAB in addition to the vibrational bands of 4-NTP, confirming the reduction of 4-NTP to *trans*-DMAB by isocyanide. We also discovered that the coverage densities of both 1,4-PDI and 4-NTP adsorbates on the Ag surface played a critical role in activating this surface-bound redox reaction. We believe that this catalytic system based on isocyanide-modified Ag as a redox catalyst can be extended to other catalytic reactions. In particular, if the characteristic SERS bands of the involved species can be well distinguished from each other, we should be able to

follow the reaction *in situ* by monitoring the changes in molecular vibrations as a function of time to gain molecular insights into the catalytic mechanisms. Nevertheless, it remains difficult to provide quantitative details about the catalytic activity, such as the yield, conversion rate, and selectivity. Part of the challenge arises from the fact that the SERS peak intensity cannot be used for any quantitative measurements.

Conflicts of interest

There are no conflicts to declare.

Acknowledgements

We acknowledge the support from the National Science Foundation (CHE-1708300) and American Chemical Society Petroleum Research Fund (PRF# 59664-ND10). Both S. S. and Y. Z. acknowledge partial financial support from Center for Organic Photonics and Electronics (COPE) at GT. We are grateful to perform the synthesis of chemicals in the laboratory of Professor Seth Marder in the School of Chemistry and Biochemistry at GT. We also acknowledge the use of the characterization facility at the Institute of Electronics and Nanotechnology (IEN) at GT.

References

1 P. Christopher and S. Linic, *J. Am. Chem. Soc.*, 2008, **130**, 11264–11265.
2 W. Huang, G. Sun and T. Cao, *Chem. Soc. Rev.*, 2017, **46**, 1977–2000.
3 P. Christopher and S. Linic, *ChemCatChem*, 2010, **2**, 78–83.
4 M. Huš and A. Hellman, *ACS Catal.*, 2019, **9**, 1183–1196.
5 G. J. K. Acres, *Platinum Met. Rev.*, 1984, **28**, 150–157.
6 J. Park, T. Kwon, J. Kim, H. Jin, H. Y. Kim, B. Kim, S. H. Joo and K. Lee, *Chem. Soc. Rev.*, 2018, **47**, 8173–8202.
7 L. Liu and A. Corma, *Chem. Rev.*, 2018, **118**, 4981–5079.
8 P. Strasser, M. Gliech, S. Kuehl and T. Moeller, *Chem. Soc. Rev.*, 2018, **47**, 715–735.
9 Z. Li, S. Ji, Y. Liu, X. Cao, S. Tian, Y. Chen, Z. Niu and Y. Li, *Chem. Rev.*, 2020, **120**, 623–682.
10 Z. Zhang, J. Ahn, J. Kim, Z. Wu and D. Qin, *Nanoscale*, 2018, **10**, 8642–8649.
11 J. Li, J. Liu, Y. Yang and D. Qin, *J. Am. Chem. Soc.*, 2015, **137**, 7039–7042.
12 J. Ahn, D. Wang, Y. Ding, J. Zhang and D. Qin, *ACS Nano*, 2018, **12**, 298–307.
13 Y. Wu, D. Su and D. Qin, *ChemNanoMat*, 2017, **3**, 245–251.
14 Y. Zhang, J. Ahn, J. Liu and D. Qin, *Chem. Mater.*, 2018, **30**, 2151–2159.
15 X. Sun, X. Yang, Y. Zhang, Y. Ding, D. Su and D. Qin, *Nanoscale*, 2017, **9**, 15107–15114.
16 H. Liu, P. Zhong, K. Liu, L. Han, H. Zheng, Y. Yin and C. Gao, *Chem. Sci.*, 2018, **9**, 398–404.
17 W. Xie and S. Schlücker, *Chem. Commun.*, 2018, **54**, 2326–2336.
18 Y. Zhang, Y. Wu and D. Qin, *J. Mater. Chem. C*, 2018, **6**, 5353–5362.
19 S. Shi and D. Qin, *Angew. Chem., Int. Ed.*, 2020, **59**, 3782–3792.
20 J. Li, Y. Wu, X. Sun, J. Liu, S. A. Winget and D. Qin, *ChemNanoMat*, 2016, **2**, 786–790.
21 T.-H. Yang, Y. Shi, A. Janssen and Y. Xia, *Angew. Chem., Int. Ed.*, 2020, **59**, 2–26.
22 S. Roy, S. Roy, A. Rao, G. Devatha and P. P. Pillai, *Chem. Mater.*, 2018, **30**, 8415–8419.
23 J. Y. Park, C. Aliaga, J. R. Renzas, H. Lee and G. A. Somorjai, *Catal. Lett.*, 2009, **129**, 1–6.
24 B. Jürgens, H. Borchert, K. Ahrenstorf, P. Sonström, A. Pretorius, M. Schowalter, K. Gries, V. Zielasek, A. Rosenauer, H. Weller and M. Bäumer, *Angew. Chem., Int. Ed.*, 2008, **47**, 8946–8949.
25 Z. Fan, X. Huang, C. Tan and H. Zhang, *Chem. Sci.*, 2015, **6**, 95–111.
26 S. M. Gruenbaum, M. H. Henney, S. Kumar and S. Zou, *J. Phys. Chem. B*, 2006, **110**, 4782–4792.
27 S. J. Bae, C. Lee, I. S. Choi, C.-S. Hwang, M.-S. Gong, K. Kim and S.-W. Joo, *J. Phys. Chem. B*, 2002, **106**, 7076–7080.
28 S. Kim, K. Ihm, T.-H. Kang, S. Hwang and S.-W. Joo, *Surf. Interface Anal.*, 2005, **37**, 294–299.
29 J. J. Stapleton, T. A. Daniel, S. Uppili, O. M. Cabarcos, J. Naciri, R. Shashidhar and D. L. Allara, *Langmuir*, 2005, **21**, 11061–11070.
30 F. Haber, *Z. Elektrochem. Angew. Phys. Chem.*, 1898, **22**, 506–514.
31 F. Haber and C. Schmidt, *Z. Phys. Chem.*, 1900, **32**, 271–287.
32 H. S. Han, S. W. Han, S. W. Joo and K. Kim, *Langmu Z. Phys. Chemir*, 1999, **15**, 6868–6874.
33 J. C. Love, L. A. Estroff, J. K. Kriebel, R. G. Nuzzo and G. M. Whitesides, *Chem. Rev.*, 2005, **105**, 1103–1170.
34 J. Ahn, S. Shi, B. Vannatter and D. Qin, *J. Phys. Chem. C*, 2019, **123**, 21571–21580.
35 Y.-F. Huang, D.-Y. Wu, H.-P. Zhu, L.-B. Zhao, G.-K. Liu, B. Ren and Z.-Q. Tian, *Phys. Chem. Chem. Phys.*, 2012, **14**, 8485–8497.
36 C. M. Stuart, R. R. Frontiera and R. A. Mathies, *J. Phys. Chem. A*, 2007, **111**, 12072–12080.
37 Y. Zhang, J. Liu, J. Ahn, T.-H. Xiao, Z.-Y. Li and D. Qin, *ACS Nano*, 2017, **11**, 5080–5086.
38 A. Picard, I. Daniel, G. Montagnac and P. Oger, *Extremophiles*, 2007, **11**, 445–452.
39 S. M. Morton and L. Jensen, *J. Am. Chem. Soc.*, 2009, **131**, 4090–4098.
40 Y. Ling, W. C. Xie, G. K. Liu, R. W. Yan, D. Y. Wu and J. Tang, *Sci. Rep.*, 2016, **6**, 31981.
41 S. M. Ansar, F. S. Ameer, W. Hu, S. Zou, C. U. Pittman and D. Zhang, *Nano Lett.*, 2013, **13**, 1226–1229.
42 Y. Yang, Y. Wang, X. Zhang, G. Qi, S. Xu and W. Xu, *J. Opt.*, 2015, **17**, 075003.
43 Y. Fang, Y. Li, H. Xu and M. Sun, *Langmuir*, 2010, **26**, 7737–7746.
44 L.-B. Zhao, J.-L. Chen, M. Zhang, D.-Y. Wu and Z.-Q. Tian, *J. Phys. Chem. C*, 2015, **119**, 4949–4958.

45 A. N. Caruso, R. Rajesh and G. Gallup, *J. Phys. Chem. B*, 2004, **108**, 6910–6914.
46 R. Abuflaha and W. T. Tysoe, *Appl. Phys. A*, 2018, **124**, 784.
47 J. I. Henderson, S. Feng, T. Bein and C. P. Kubiak, *Langmuir*, 2000, **16**, 6183–6187.
48 G. Baraldi, E. Lopez-Tobar, K. Hara, S. Sanchez-Cortes and J. Gonzalo, *J. Phys. Chem. C*, 2014, **118**, 4680–4686.